https://doi.org/10.26599/SES.2025.9590020

Research Article

Experimental study on cable combustion and smoke propagation in confined underground environments

Chang Liu✉, Peng Li, Kunpeng Ji, Jingshan Han

State Grid Electric Power Engineering Research Institute, Beijing 100192, China

✉ Corresponding author. E-mail: liuchang.2019@tsinghua.org.cn

Received: December 13, 2025; Revised: December 23, 2025; Accepted: December 24, 2025

Abstract: Full-scale fire tests were conducted in a 331 m long urban underground cable tunnel to investigate how fire source area, cable layer number, and spatial arrangement jointly affect combustion, temperature evolution, and smoke toxicity. Eleven Case were designed by varying fuel tray area and volume, cable layers (0–5), and multilayer versus dense single-layer layouts. Enlarging the fire source significantly increased the mass loss rate and total fuel consumption, indicating stronger combustion. More cable layers raised ceiling peak temperature and prolonged high-temperature duration due to enhanced heat feedback. Stratified multilayer cables produced a stable high-temperature ceiling zone, whereas dense single-layer cables caused rapid heating but lower peaks and faster cooling because of local oxygen depletion. Higher cable load and denser layouts markedly reduced visibility and increased CO concentration and persistence. These findings deepen the understanding of fire behavior in urban underground cable tunnels and provide a scientific basis for optimizing safety design and emergency response strategies.

Keywords: Cable tunnel; Full-scale fire experiments; Temperature distribution; CO concentration.

1.Introduction

With the accelerated pace of urbanization, the demand for electrical power in cities continues to grow. Underground cable tunnels, as critical infrastructure for ensuring urban energy supply, are of paramount importance to operational safety. These tunnels are typically characterized by confined and elongated spaces, high cable density, and limited ventilation, resulting in a high fire risk. Once a fire occurs, it can easily lead to rapid flame spread, intense heat accumulation, and the diffusion of toxic smoke, posing severe threats to urban operations and personnel safety. An et al. (2024), through numerical simulations, found that while increasing the sealing ratio can shorten the overall burning duration, it accelerates the spread of high-temperature zones. J. Zhang et al. (2025) demonstrated that an increase in tunnel slope enhances the stack effect, significantly increasing flame spread distance and rate. T. Zhang et al. (2025) developed a coupled atmospheric pressure-interlayer spacing model, indicating that reduced atmospheric pressure in high-altitude regions significantly inhibits flame spread. Therefore, systematically investigating the combustion characteristics and smoke spread patterns in cable tunnel fires is crucial for enhancing the disaster prevention and mitigation capabilities of urban power systems.

Significant progress has been made in understanding fire-induced smoke movement and temperature distribution. Zhao et al. (2018), through reduced-scale experiments, revealed the significant influence of radiation from the smoke layer on ceiling temperature and found that temperature decays exponentially along the tunnel longitudinal axis. Liu et al. (2025), based on full-scale tests, categorized cable fire spread into three modes: "no spread — longitudinal — vertical," with the transition threshold depending on ignition energy and heat exposure time. An et al. (2021) identified a critical longitudinal ventilation velocity (0.45 m/s) at which the ceiling temperature response undergoes a distinct transition. Liang et al. (2019) and Huang et al. (2024) investigated the influence of T-shaped tunnel junctions and spatial dimensions on smoke flow paths and temperature distribution using numerical simulations and small-scale experiments, respectively. However, systematic experimental data under multi-variable coupling Cases remain relatively scarce.

Cable arrangement is a key factor influencing fire spread behavior. M. Liu et al. (2025) found that flame height and mass loss rate peaked when the cable spacing was equal to one cable diameter. Xu et al. (2025; 2023) showed that an interlayer spacing of less than 1 cm easily leads to a "mutual heating effect," causing a significant increase in the heat release rate. An et al. (2020) and Wang et al. (2025) further explored the nonlinear effects of interlayer spacing, cable spacing, and aging time on flame spread rate and combustion characteristics. Furthermore, Bai (2024) and Zheng et al. (2023), using experimental tools such as the cone calorimeter, revealed significant differences in ignition time, heat release rate, and smoke toxicity among different cable materials. Most of the studies are based on reduced-scale experiments, and the applicability of their conclusions in full-scale complex environments requires further verification. The full-scale experiments by C. Wang et al. (2025) confirmed that the combustion of multiple cable layers can cause a rapid rise in ceiling temperature accompanied by substantial CO generation within a short time. T. Wang and An (2023) and T. Wang et al. (2024) emphasized the coupled effects of multiple factors, including longitudinal ventilation, cable spacing, number of layers, and initial ignition location, on flame morphology and heat release rate.

In summary, although existing research has made significant progress in understanding temperature distribution, smoke diffusion, and fire spread mechanisms, the following shortcomings remain: 1. There is a lack of systematic full-scale experimental studies that comprehensively consider the combined effects of fire source area, number of cable layers, and arrangement; 2. The dynamic coupling relationships between mass loss, flame temperature, ceiling temperature rise, and smoke concentration are not yet clear; 3. Most existing models are based on reduced-scale experiments or single-variable assumptions, and their applicability needs further verification under full-scale Cases. To address these gaps, this paper conducts full-scale fire experiments in an urban underground cable tunnel in China. Different combinations of fire source area and number of cable layers are established, and key parameters including mass loss, flame temperature, ceiling temperature rise, and CO concentration are synchronously collected to analyze their coupled evolution. This study aims to provide data support and a theoretical basis for fire risk assessment and the optimization of fire protection design in urban cable tunnels.

2. Experimental Methodology

2.1Experimental Overview

This full-scale experiment was conducted in an underground cable tunnel in a Chinese city to investigate cable fire spread characteristics and their impact on the tunnel environment. The selected tunnel is representative of typical urban underground cable transmission passages, featuring a regular internal structure and a relatively narrow, elongated space. Multi-tier cable brackets support the power cables within. During all tests, both tunnel portals were sealed, and longitudinal exchange through the portals was negligible. Ventilation was provided only by buoyancy-driven natural ventilation through a vertical shaft connected to the cable tunnel. No mechanical ventilation or forced smoke extraction was applied while monitoring equipment installed on the ceiling and sidewalls recorded temperature variations, carbon monoxide (CO) concentrations, and smoke flow dynamics in real-time during the fire. The experiment involved igniting cables at predetermined locations to document flame spread, hot smoke production, and diffusion patterns, thereby providing critical data for fire prevention and control strategies. The tunnel was equipped with a modern monitoring system and fire-retardant coatings to ensure experimental safety and data accuracy, establishing an empirical foundation for numerical simulation of urban cable tunnel fires and disaster mitigation research.

2.2 Experimental Design

As shown in Figure 1, the test cable tunnel section is arranged horizontally with a total length of 331 meters. Cable supports are spaced 1 meter apart horizontally across five layers. Both ends of the tunnel are sealed, relying solely on ventilation shafts for smoke extraction. Temperature measurement was performed using a hybrid system, enabling real-time distributed temperature measurement of flames and smoke throughout the test. This system comprised: - Distributed Fiber Optic Temperature Sensing (DTS), capturing the temperature field above the flame/fire source; - Thermocouple bundles, primarily measuring smoke temperatures in the vertical direction. Ten thermocouple bundles, labeled T1-T10, were vertically arranged along the tunnel's longitudinal axis with approximately 0.15-meter spacing between adjacent points. The ignition source was positioned between thermocouple bundles #6 and #7, with 3 meters of clearance on either side. The remaining 30 thermocouple bundles were spaced 5 meters apart.

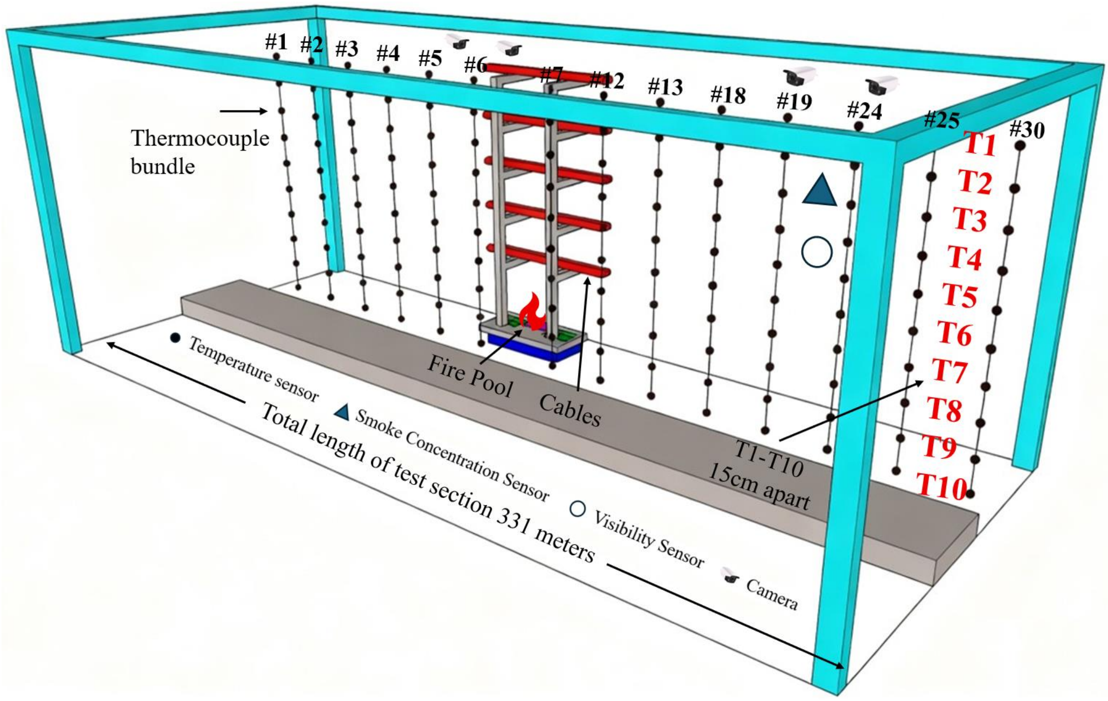

Fig. 1. Horizontal layout of test cable tunnels and temperature measurement lines

Figure 2 illustrates the cable layout for levels L1 to L6. A protective layer is installed on the tunnel ceiling, with a balance mounted to measure mass loss before and after combustion. Gas analyzers are mounted on sidewall cable brackets, positioned 6 meters horizontally from the fire source. These devices measure flue gas composition, harmful gas concentrations, and smoke dispersion rates.

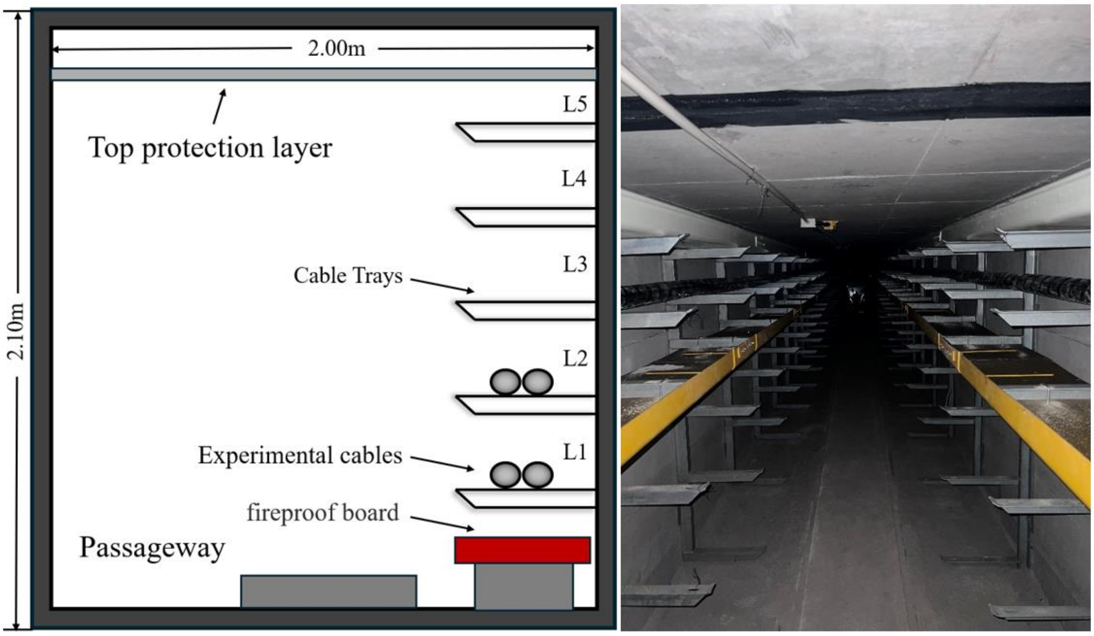

Fig. 2. Schematic cross-section of cable tunnel (unit: m)

2.3 Test Cases

As summarized in Table 1, eleven test cases were designed. These include variations in the number of cable layers (from 2 to 5 layers) for fire source areas of 1500 cm^2 and 3400 cm^2, respectively, along with control groups involving bare combustion (without any cables).

Table 1 Test cases

Case No.	Fire source area/cm^2	Fuel volume/L	No. of cables /per layer	Number of cables	Cable present or absent
1	1500	3	2	2	present
2	3400	6.8	2	2	present
3	1500	3	2	4	present

4	1500	3	2	6	present
5	3400	6.8	2	4	present
6	3400	6.8	2	6	present
7	3400	6.8	2	8	present
8	3400	6.8	2	10	present
9	3400	6.8	3	6	present
10	1500	3	2	0	absent
11	3400	6.8	2	0	absent

2.4 Test Cases

Figure 3 shows the operating Cases during the cable combustion test. Within approximately 20 seconds of the fire's onset, the bottom layer of cables ignited, with flames confined near the ignition point. Subsequently, the flames spread laterally along the bottom layer cables and gradually ignited the second layer of cables above, forming a vertical flame plume. By approximately 200–400 seconds, the third and fourth layers of cables were successively ignited. The flame height increased significantly, reaching the tunnel ceiling, while flame intensity rapidly escalated as more fuel became involved. Concurrently, substantial smoke accumulated beneath the ceiling and dispersed along the tunnel axis. Visibility near the fire source deteriorated sharply around 600–800 seconds, while distant areas experienced significantly reduced visibility as the smoke layer settled. Structurally, temperatures in the tunnel lining and cable supports continued to rise; prolonged exposure to high temperatures could cause strength degradation or deformation in the supports.

Compared to the two-layer cable scenario, the four-layer cable fire spreads more rapidly and exhibits three-dimensional expansion. The “chimney effect” generated by the multi-layer arrangement accelerates vertical flame propagation, resulting in greater flame height and heat release rates. Due to the increased total combustible mass, the four-layer cable fire produces denser smoke, causing more severe and earlier visibility reduction. Overall, both combustion intensity and propagation efficiency exceed those of the two-layer cable scenario, posing more severe challenges to tunnel structures and the surrounding environment.

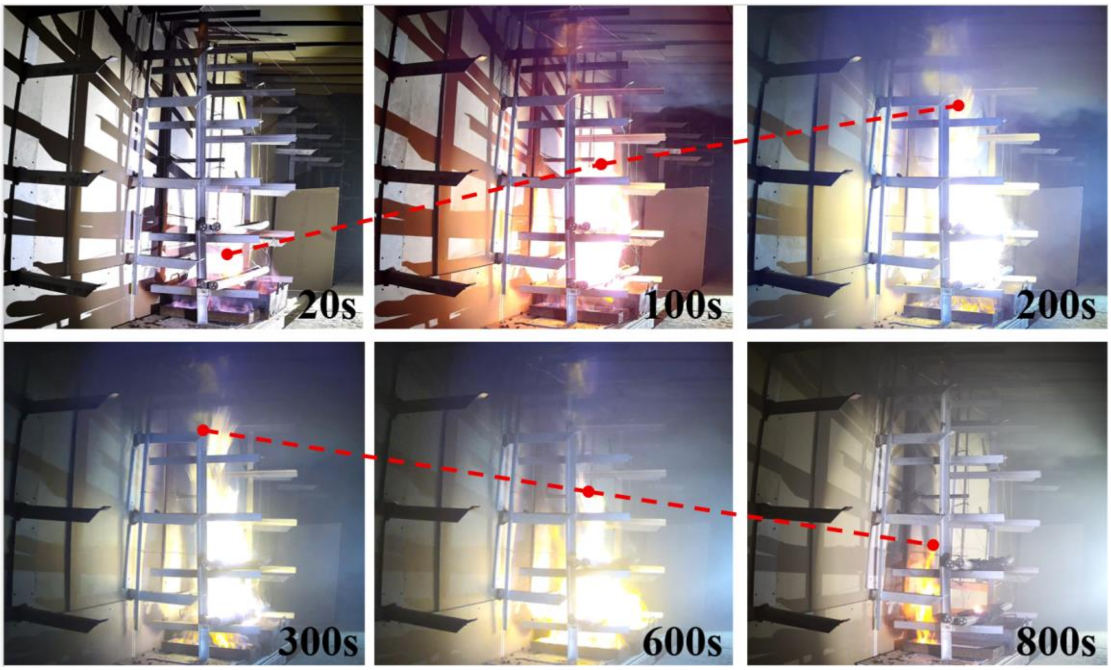

(a) Two cables per floor, totaling two floors

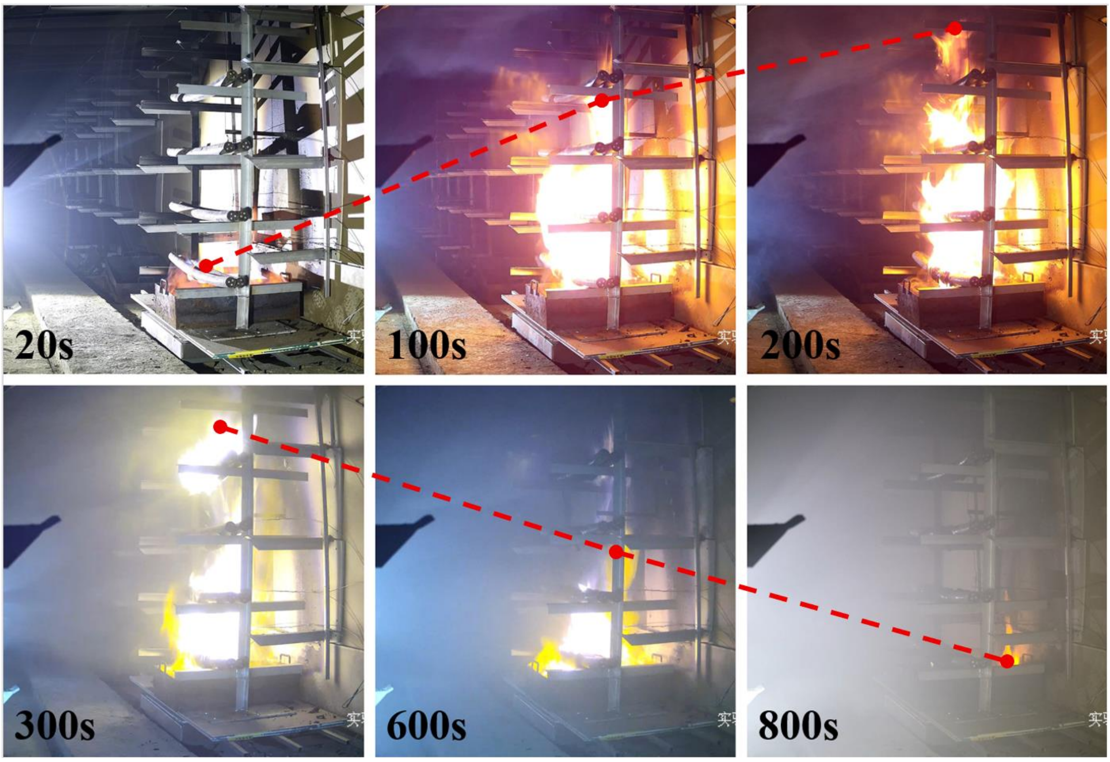

(b) Two cables per floor, totaling four floors

Fig. 3. Cable Combustion Test Cases in Underground Cable Tunnels Under Different Operating Cases

3.Experimental Results and Discussion

3.1 Mass Loss

As illustrated in Fig. 4, analysis of the mass loss versus time curves for identical cable arrangements under different fire source areas reveals that the descent amplitude of the mass loss curve for Case 6 consistently exceeds that of Case 4. The final mass loss reached 6.47 kg for Case 6, compared to only 2.72 kg for Case 4, with the former being approximately 2.4 times the latter. This indicates that, under identical cable arrangement cases, increasing the fire source area from 3 cm^2 to 6.8 cm^2 significantly intensified the combustion reaction. Furthermore, from a temporal perspective, the mass loss rate of Case 6 continuously remained higher than that of Case 4 within the first minute, further validating the promoting effect of a larger fire source area on both the sustainability and intensity of combustion. The analysis of mass loss over time under identical fire source area but different cable arrangements reveal the following final mass losses: Case 2:5.79 kg; Case 5:6.175 kg; Case 6:6.47 kg. Although the fire source area remains constant across these three cases, the total mass loss progressively increases as the number of cable layers rises from one layer (Case 2) to two layers (Case 5) and further to three layers (Case 6). Each additional cable layer contributes to a greater mass loss. This indicates that a higher number of cables provides a greater total combustible load, leading to more combustion and consequently more significant mass loss.

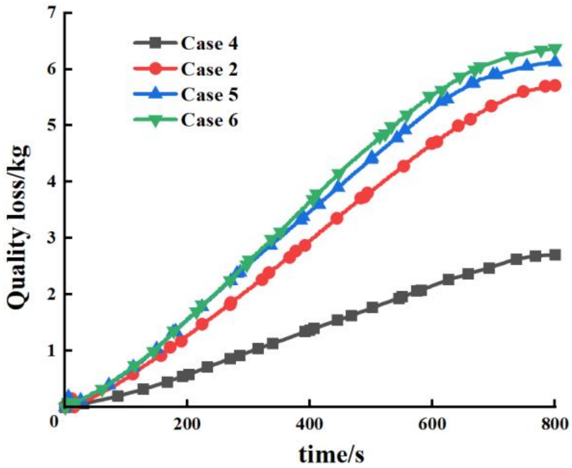

Fig. 4. Mass loss overtime for identical cables under different fire source area cases

As depicted in Fig. 5, the mass loss rate data reveal that all three cases exhibit a consistent trend: rapid initial increase, peak attainment during mid-phase, and gradual decline in the later stage. However, distinct differences are observed: Case 6 demonstrates the highest peak rate of 11.21 g/s, maintained for a prolonged duration, indicating the most intense combustion. Case 5 reaches a slightly lower peak of 10.38 g/s compared to Case 6 but also sustains elevated values for an extended period. In contrast, Case 2 attains a peak rate of only 9.48 g/s with a relatively short duration of high values, reflecting comparatively moderate combustion. Furthermore, during the descending phase of the rate curves, Case 6 shows the slowest decay rate, suggesting sustained higher reactivity even in the later stages of combustion.

This analysis demonstrates that under identical fire source area cases, the number of cable layers significantly influences combustion intensity and duration. A greater number of cable layers corresponds to more intense combustion, higher peak mass loss rates, prolonged maintenance of high combustion states, and slower decay in the later stages.

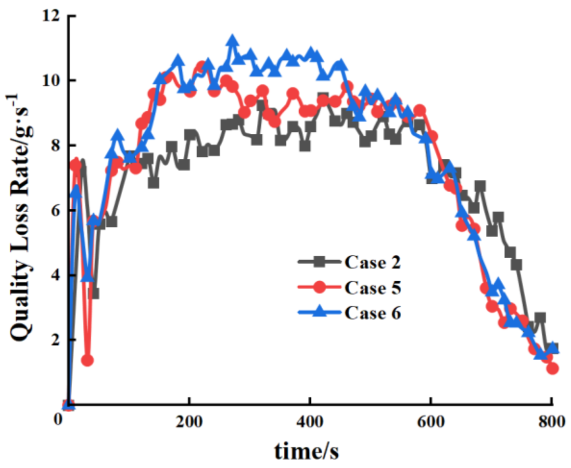

Fig. 5. Mass loss rate over time for the same fire source area under different cable arrangements

3.2 Flame Temperature

Under all experimental cases, the temperature curves recorded at the measurement points exhibit a typical fire development process: rapid initial temperature rise, attainment of a peak, followed by a gradual cooling phase. This indicates that the cable fires rapidly progress to flashover after ignition. After reaching the maximum temperature, the combustion intensity gradually diminishes as the combustible material is consumed. Across all cases, Measurement Point 1, being closest to the fire center, consistently recorded the highest flame temperature within its respective case, most accurately reflecting the core combustion intensity.

The flame temperature data for Case 2 show that the flame entered an intense combustion stage shortly after ignition. The temperature at Point 1, nearest to the fire source, surged from 26.5°C to 104.8°C within 3 seconds, reaching a peak of approximately 844.2°C around 400 seconds. During the mid-phase of combustion (approximately 50-600 seconds), temperatures at all points fluctuated within a high range, demonstrating dynamic instability of the combustion process. A clear temperature gradient was observed, with a peak temperature difference of about 800°C between the nearest and farthest points. In the later stage, temperatures decreased slowly, with points near the fire source maintaining temperatures above 700°C for about 300 seconds. This indicates high combustion intensity and persistent heat release in this case, overall presenting a three-stage combustion characteristic: rapid temperature rise, sustained high temperature, and slow cooling, providing crucial data support for combustion efficiency assessment and thermal system design.

While the peak temperature at Point 1 was identical (881°C) in both Case 6 and Case 2, the heating process and overall temperature levels in Case 6 were significantly higher during many periods. During the mid and late combustion stages, temperatures in Case 6 were generally 20-50°C higher than those in Case 2. This phenomenon is attributed to the greater number of cable layers in Case 6 compared to Case 2, leading to more sustained combustion and greater total heat release, thereby maintaining a higher overall temperature level.

The flame temperature data for Case 9 indicate that the flame entered an intense combustion stage rapidly after ignition. The temperature at Point 1, closest to the fire source, rose sharply from 21.5°C to nearly 800°C within approximately 250 seconds, maintaining high temperatures with fluctuations during the early to mid-phase (around 200–600 seconds), reaching a maximum of about 799°C. The temperatures during combustion showed significant spatial decay, with a peak temperature difference exceeding 600°C between the nearest (Point 1) and farthest (Point 6) points, reflecting strong thermal distribution non-uniformity. In the later stage (approximately 800–1200 seconds), temperatures gradually decreased overall, eventually returning to ambient levels of 30–40°C.

Under cases of identical total fuel load and cable quantity, Case 6 and Case 9 exhibited significant differences in combustion characteristics due to different cable arrangements. In Case 6, the greater number of cable layers and more dispersed spatial distribution enhanced resistance to flame spread, resulting in more concentrated combustion, higher peak temperatures, and longer duration of high temperatures. In contrast, Case 9, employing a denser single-layer arrangement, promoted air circulation and combustion efficiency, manifesting as a faster initial temperature rise and more pronounced fluctuations in heat release during the mid-phase, but ultimately lower overall temperature levels and faster cooling. This reveals the crucial regulatory role of cable spatial layout on the combustion process.

Comparative analysis of the temperature curves from six different measurement locations across all cases demonstrates that: increased fuel load enhances fire source power, leading to more complete combustion and a more uniform temperature field; an increase in the number of cables significantly raises the total heat release, increasing the overall temperature level and prolonging the duration of high temperatures. Under cases of the same total number of cables, the arrangement becomes a key influencing factor: a layered, dispersed structure achieves more concentrated combustion and higher peak temperatures by enhancing flame spread resistance, whereas a single-layer, dense arrangement accelerates the heating rate by promoting air flow but limits temperature accumulation. This reveals the coupled mechanism by which fuel load, cable quantity, and spatial layout jointly regulate combustion intensity and heat release characteristics.

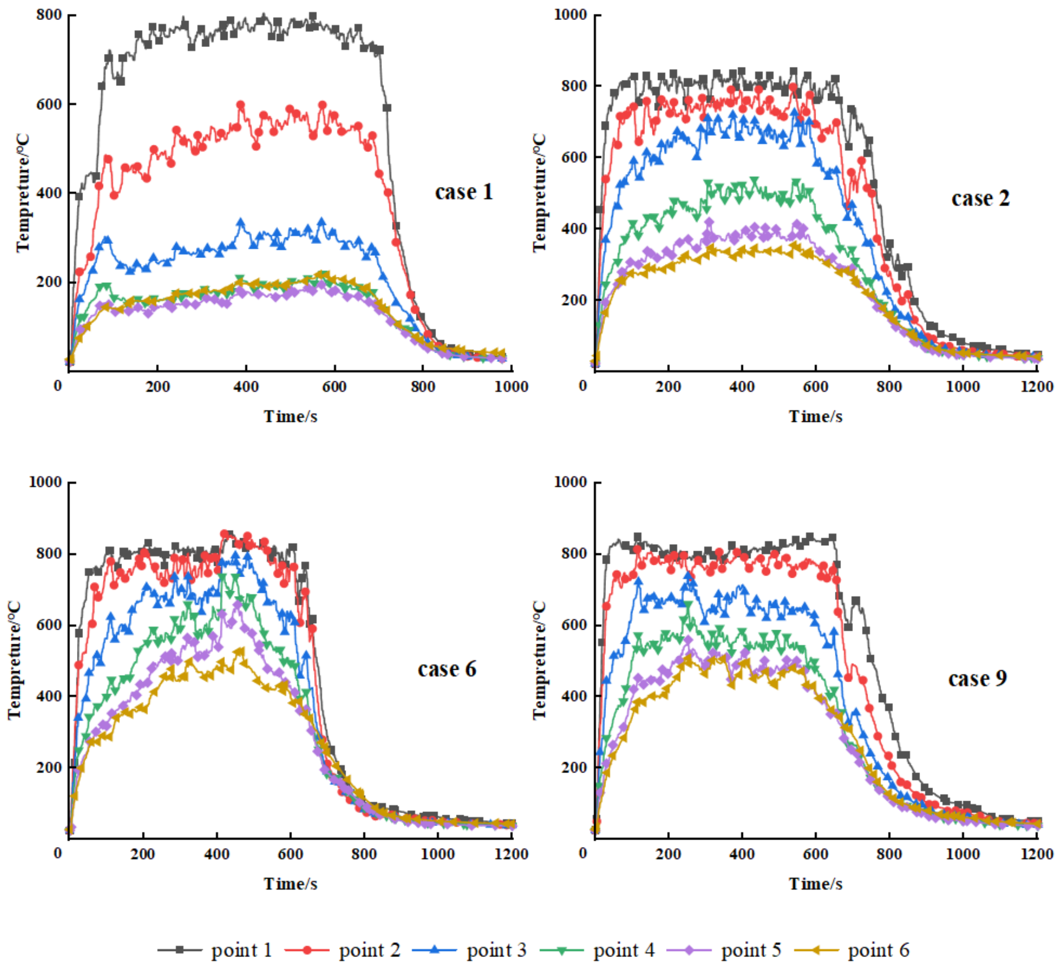

Fig. 6. Temperature of the flame over time under different operating cases

3.3 Temperature at Measurement Points

3.3.1 Ceiling Temperature

Ceiling temperature is a critical parameter for evaluating the characteristics of smoke layers in tunnel fires, the severity of thermal hazards, and the effectiveness of smoke exhaust systems. Based on the experimental cases designed, we compared the patterns of ceiling temperature variation under different variables such as fire source area, number of cable layers, and cable arrangement methods. In this experiment, the temperature measured at point #7-T1, located to the right of the fire source, was adopted as the ceiling temperature value. The figure illustrates the temporal evolution of ceiling temperature across four operational cases during the model experiments.

Comprehensive analysis of the canopy temperature data reveals significantly divergent thermal evolution patterns across the four operating cases: 11 exhibits the most gradual temperature rise curve, climbing steadily from an initial 29.3°C to reach a moderate peak of 105.1°C at approximately 450 seconds. The entire heating process remains uniform and stable, ultimately cooling down to around 50°C. This trend clearly delineates the thermal boundary of pure fuel combustion. Its limited thermal output and slow thermal dynamics provide a crucial benchmark for other operating cases involving cables. Operating case 6 exhibits typical characteristics of highly efficient and stable combustion. Its temperature curve rises rapidly during the initial 0-100 seconds, maintains a steady upward slope in the middle phase, and reaches a peak of 111.1°C at approximately 430 seconds. Most notably, it enters an extended high-temperature plateau lasting nearly 400 seconds, with minimal fluctuations (<3°C) between 105-111°C, demonstrating exceptional thermal stability and inertia. The experiment concludes at a maximum equilibrium temperature of 40.3°C. This trend indicates that a stratified, dispersed cable layout can establish a persistent, stable combustion environment, maximizing the thermal accumulation effect of the ceiling. case 8 exhibited violent and unstable thermal behavior. Its heating rate was the fastest overall, reaching a peak of 118.3°C at approximately 450 seconds. However, the post-peak cooling phase exhibited pronounced temperature fluctuations and oscillations, reflecting instability in the combustion process or smoke layer. This trend correlates closely with its highest combustible material quantity and strongest “chimney effect,” which, while yielding an extremely high heat release rate, also intensified combustion turbulence and reduced stability. case 9 provides the most intriguing comparative case. Despite identical cable counts to case 6, its thermal behavior diverged markedly: the heating curve remained consistently below case 6, with an earlier and lower peak of 105.6°C. Notably, the post-peak cooling rate was exceptionally steep, ultimately converging to temperatures comparable with case 8. This pattern reveals the complex influence of dense cable arrangements on thermal dynamics—simultaneously limiting combustion intensity while significantly enhancing late-stage heat dissipation efficiency.

The power of the ignition source governs the peak temperature and initial heating rate, as demonstrated in Scenario 8; whereas the spatial geometric layout of the cables dominates the heat release pattern, process stability, and system thermal inertia. A dispersed multi-layer arrangement is most conducive to establishing a persistent, stable environment, leading to severe heat accumulation. Conversely, a dense, few-layer arrangement, while participating in combustion, results in a more rapid cooling process.

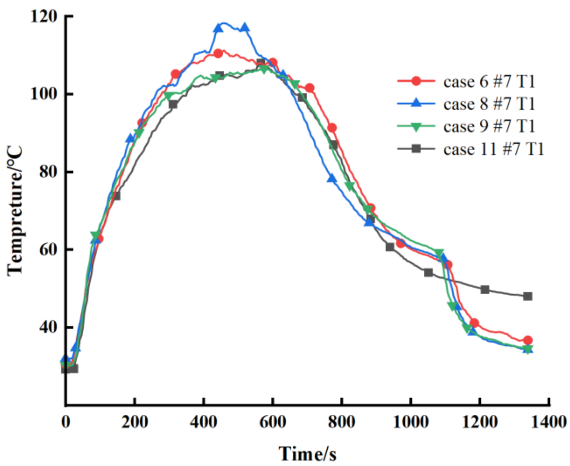

Fig. 7. Changes in ceiling temperature over time under different operating cases

3.3.2 Longitudinal Temperature

As shown in Fig. 8, temperature points #7T1, T3, and T5 vary over time under different operating cases. Through in-depth analysis combining temperature data with operating parameters, the following patterns can be summarized. Operating case 2 exhibits typical constrained combustion characteristics, with T1 rising slowly from an initial 29.3°C, reaching a peak of 107.9°C between 560-570 seconds. The entire heating process is stable without significant fluctuations, and the cooling rate after the peak is slow. By the end of the test, it remains at approximately 52°C, reflecting the inherent nature of weak combustion intensity and sustained but low-level heat release under cases of low fuel load and small heat source. case 6 exhibited typical complete combustion behavior, with T1 rapidly climbing from 30.7°C to reach its first peak of 110.1°C between 410–420 seconds. followed by multiple ±2°C temperature oscillations between 300-500 seconds, indicating combustion instability. Subsequently, a high-temperature plateau formed in the 90-100°C range, persisting until a significant decline after 650 seconds. This demonstrates that high fuel quantity combined with moderate cable configuration promotes sustained combustion. T1 rapidly increased from 32.1°C, reaching the highest peak of 118.3°C between 440-450 seconds. The high-temperature phase (>110°C) persisted for nearly 200 seconds, remaining above 97°C until 700 seconds. This demonstrates that increasing the number of cable layers significantly enhances combustible surface area and ventilation efficiency, leading to more complete and intense combustion. case 9, however, exhibits a “high load, low efficiency” phenomenon. Although the initial temperature rise is rapid, with T1 reaching 53.3°C within 32 seconds, the peak is only 106.7°C. Moreover, the temperature drops precipitously after the peak, plummeting from 106°C to 68°C within 300 seconds. This reveals that an excessively dense cable arrangement causes a flame suffocation effect, limiting combustion integrity. Overall, fuel quantity and flame source areas establish the foundation for combustion potential, while cable structure remains the key regulator of combustion efficiency. Increased layer count enhances combustion intensity by boosting air entrainment, whereas higher density inhibits combustion development by hindering oxygen diffusion. This contradictory relationship precisely explains the fundamental differences in temperature curves across operating cases.

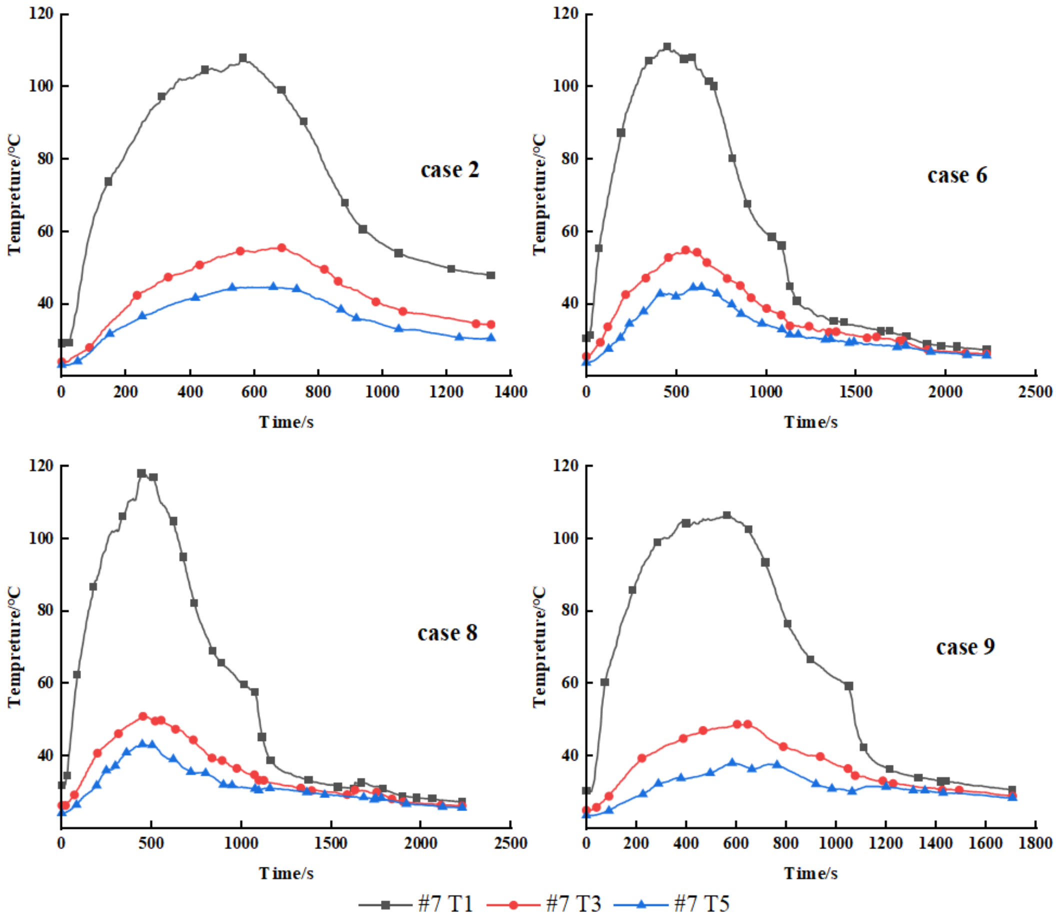

Fig. 8. Temperature measurement points over time under different operating cases

3.4 Visibility

As shown in Fig. 9, the visibility time-series data and corresponding operating case parameters are presented. Visibility-time curves for all operating cases generally exhibit the following pattern: visibility approaches 1 at approximately 70 – 100 seconds initially, then gradually decreases as combustion progresses and smoke accumulates. Significant differences exist among cases in the onset time of decay, minimum visibility, and duration of low visibility. Observing case 2, 4, 6, 8, and 9: In Scenario 2, where the fuel volume was 3400 L and only 2 cables were deployed, visibility began to decline slowly after approximately 100 seconds. The minimum value remained around

0.65 and never fell below 0.5 throughout the process. This indicates that under cases of relatively low combustible cable load, smoke generation is limited. maintaining relatively high visibility throughout the cable tunnel. In Scenario 4, despite reducing fuel volume to 1500 L, increasing the number of cables to 6 caused visibility to gradually decline to approximately 0.40 during the middle and late stages, remaining below 0.5 for an extended period. This demonstrates that the increased combustible material from the cables sufficiently counteracts the reduced fuel volume, significantly elevating smoke concentration. In case 6, maintaining 6 cables under 3400 L fuel, visibility declined more rapidly, dropping below 0.7 within approximately 100 seconds. It subsequently fluctuated within the 0.3 – 0.6 range for an extended period, reflecting the synergistic effects of higher heat release rates and cable combustion, which simultaneously intensified smoke generation and obscuration. Under the same fuel cases, Scenario 8 increased the number of cables to 10. Visibility dropped below 0.5 around 150 seconds, subsequently falling below 0.3 and 0.2, with a minimum value approaching 0.03. The prolonged period of extremely low visibility characterized this scenario as the most unfavorable for evacuation and visibility. Comparing Scenario 9 (3400 L, 6 cables arranged 3 per layer) with Scenario 6 (3400 L, 6 cables arranged 2 per layer), the former exhibits earlier and more rapid visibility decline, with a minimum value around 0.20. The duration below 0.5 is significantly shorter, while the period below 0.2 is notably longer. It is evident that visibility in Scenario 9 begins to decline rapidly at an earlier stage, reaching a minimum of approximately 0.20, with a significantly longer duration below 0.5. This indicates that increasing cable density within a layer and altering spatial arrangements can substantially exacerbate localized smoke retention and visual obstruction, even when the total number of cables remains constant. Comprehensive comparison of different fuel quantities, fire source areas, and cable quantities/arrangements suggests that fuel heat release intensity and cable combustible load jointly determine the temporal evolution of visibility. Notably, increased cable quantity and concentrated arrangement significantly amplify visibility decay, revealing an overall trend: “Higher fuel loads and denser cables result in faster visibility decline, lower minimum values, and prolonged periods of low visibility.”

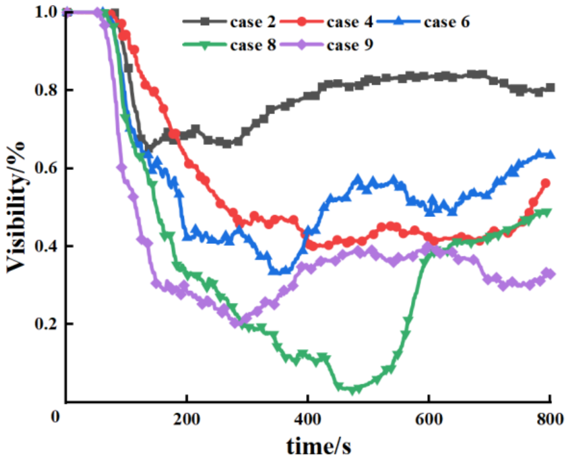

Fig. 9. Visibility variation over time under different operating cases

3.5 CO concentration

As shown in Fig. 10, this study comparatively analyzed the dynamic evolution of CO concentrations across four operating cases from 0 to 1000 seconds, revealing significant temporal differences and distribution characteristics. case 10 (no cable) consistently maintained a low concentration of approximately 32–55 ppm with relatively stable behavior. case 1 (single-layer cable) exhibited the fastest concentration rise rate within the first 200 s, followed by a decrease between 200–600 s. It then recovered to around 78 ppm before initiating a rapid decline after approximately 800 s. case 3 showed a gradual CO concentration increase before approximately 270 seconds, peaking at around 80 ppm at this time. Subsequently, it entered a phase of fluctuating between 60–

80 ppm after an initial decrease followed by an increase, gradually decaying after approximately 750 seconds; Under case 4, CO concentration surged to a peak of approximately 110 ppm around 400 s, then dropped to about 60 ppm around 600 s. After a minor rebound, it began a sustained decline starting at 670 s. At 1000 s, Operating case 10 exhibited the highest CO concentration among the four cases, while case 4 showed the lowest. This temporal pattern indicates that cable arrangement and combustion evolution decisively influence the time spectrum of CO generation. Furthermore, the instantaneous peak and subsequent concentration recovery/decay behavior may be jointly governed by coupled factors such as localized oxygen supply, thermal inertia, and combustion persistence.

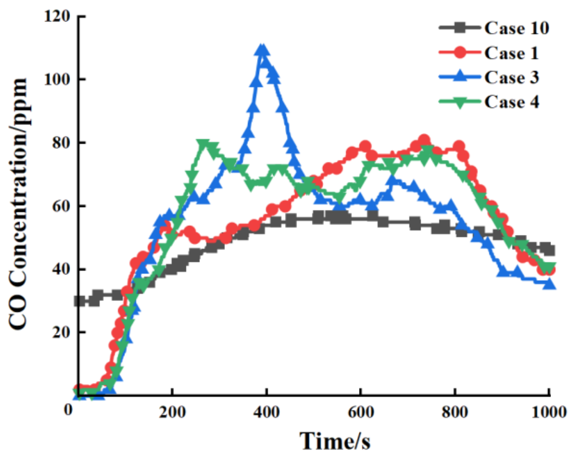

Fig. 10. Trend of CO Concentration Over Time for Different Cable Quantities

As shown in Fig. 11, the CO concentration data for Operating cases 4, 6, and 9 exhibit distinct patterned variations closely related to fuel volume, fire source area, and cable arrangement. Under Operating case 4, CO concentrations consistently remain at low levels. The initial baseline is approximately 1–2 ppm, rising slowly after about 550 seconds before peaking at around 80 ppm between 732–741 seconds and sustaining this level for approximately 10 seconds. Following the peak, CO concentration gradually declines to a low value at the end of the test. The average CO concentration in case 4 was approximately 36.8 ppm, significantly lower than other cases, indicating a more complete combustion process with a gradual fire growth rate. The CO concentration in case 6 was significantly higher overall than in cases 4 and 9. The initial CO concentration was approximately 5 ppm, rapidly rising to exceed 10 ppm after about 109 seconds. It peaked at 240 ppm around 503 seconds, the highest among the three operating cases. Following the peak, the CO concentration remained elevated for several hundred seconds before gradually decreasing in the later stages. Operating case 6 exhibited an average CO concentration of approximately 117.6 ppm, indicating high combustion intensity coupled with insufficient oxygen supply, resulting in substantial CO production. The CO concentration variation in operating case 9 fell between that of cases 4 and 6. Initial CO concentrations also remained around 1 ppm, exceeding 10 ppm at approximately 210 seconds, followed by a peak of about 227 ppm between 462–465 seconds. Post-peak CO concentrations declined gradually but remained higher overall than in case 4. Operating case 9 exhibits an average CO concentration of approximately 100.6 ppm. Both the peak and average CO values are higher than those of operating case 4 and slightly lower than those of operating case 6, indicating that the intensity of combustion is second only to operating case 6.

Based on the above analysis, CO data from three typical operating cases reveals distinct patterns in fire intensity and ventilation cases: case 6 produced the highest CO levels with the longest duration, indicating the most intense combustion and oxygen deficiency. case 9 showed intermediate levels, while case 4 exhibited the lowest. High CO peaks and early onset correspond to more intense incomplete combustion processes, while low CO concentrations indicate more complete combustion. Overall, harsher fire cases (abundant fuel or restricted ventilation) result in higher combustion intensity and greater heat release but also increased CO emissions; under milder cases, combustion is more complete and CO production is reduced. These systematic patterns provide important indicators for assessing fire development stages.

Under identical total cable cases, increased fuel volume significantly accelerates CO accumulation rates and markedly shifts peaks upward: CO peak at operating case 6 reached approximately 240 ppm (peak duration ~503 s, average ≈117.6 ppm), while operating case 9 reached a peak of approximately 227 ppm (peak duration: approx. 462–465 s, average: ≈100.6 ppm). In contrast, operating case 4 with a smaller fuel volume exhibited a peak of only about 80 ppm (peak duration: approx. 732–741 s, average: ≈36.8 ppm). Further comparison between Operating case 6 and 9 reveals that despite identical total root counts, the multi-layer vertical stacking in case 6 exhibits higher CO generation and a longer high-concentration maintenance period. This suggests that, at equivalent total mass-to-volume ratios, increased vertical stacking density is more detrimental to local ventilation and exacerbates thermal feedback and incomplete combustion.

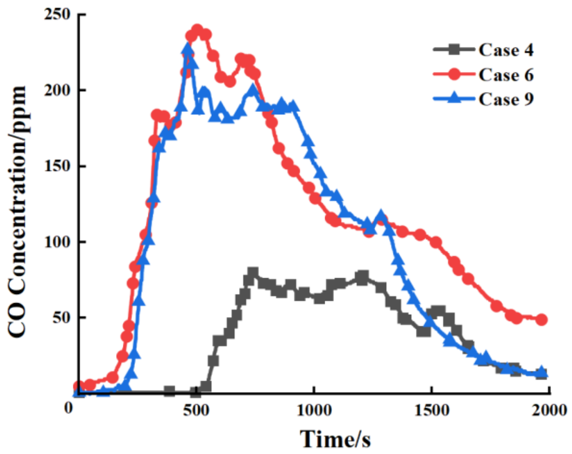

Fig. 11. Trend of CO Concentration Over Time for Different Fire Source Areas

4. Conclusion

Based on systematic research from full-scale fire experiments, this paper conducts an in-depth analysis of the influence patterns of fire source area, cable layer count, and arrangement methods on combustion characteristics, temperature field evolution, and toxic gas distribution in cable tunnel fires. The following key conclusions are drawn:

(1) Both the fire source area and the number of cable layers jointly regulate the combustion intensity and heat release pattern. Experimental data show that increasing the fire source area from 3 L to 6.8 L elevates the peak mass loss rate by 18.3% and increases the total mass loss by approximately 2.4 times. Increasing the number of cable layers from 1 to 3 elevated the peak ceiling temperature from 107.9°C to 118.3°C, prolonging the high-temperature duration by nearly 200 seconds. The multi-layer cable structure enhances thermal radiation and heat feedback effects, creating a positive feedback mechanism for combustion that significantly exacerbates flame propagation risks. It is recommended to control the density of single-layer cables during actual cable installation and to install vertical fire barriers to suppress vertical heat accumulation. This series of data patterns confirms the positive correlation between energy release and combustible load. It also reveals that the confined space structure formed by multi-layer cables accelerates fire spread through positive feedback by enhancing the radiant preheating of unburned cables via the heat and smoke layer.

(2) Cable arrangement patterns govern combustion stability and temperature field distribution. The stratified, dispersed layout formed a sustained high-temperature plateau on the ceiling lasting approximately 400 seconds, with temperature fluctuations below 3°C, demonstrating excellent thermal inertia. In contrast, the single-layer, dense arrangement exhibited faster initial heating but resulted in a 5% reduction in peak temperature, followed by a “cliff-like” drop during the cooling phase. This comparative pattern confirms, from combustion theory, that layered arrangement enhances combustion stability by optimizing fuel distribution. Conversely, dense arrangement

triggers a shift from ventilation-controlled to fuel-controlled combustion due to localized oxygen depletion. Together, these mechanisms elucidate the nonlinear influence of cable layout on fire progression. In cable tunnel design, layered, dispersed arrangement should be prioritized to mitigate the risk of sudden fire spread.

(3) The evolution of visibility and CO concentrations reflects fire toxicity risks and combustion completeness. As the number of cable layers increases, peak smoke concentrations rise over fourfold, while peak CO concentrations surge from 80 ppm to 240 ppm—a threefold increase. Under identical total cable quantities, multi-layer configurations exhibited approximately 14.5% higher average CO concentrations than single-layer arrangements, with significantly prolonged periods of elevated concentrations. These precise data patterns theoretically confirm that CO generation dynamics are governed by the spatiotemporal distribution of oxygen concentration and temperature fields within combustion zones. The phenomenon of earlier peak concentrations and sustained high values serves as a critical indicator for assessing fire hazards and evaluating ventilation system effectiveness.

This study is based on full-scale tests conducted under a specific tunnel geometry and ventilation boundary condition, and the conclusions should be interpreted within this scope. In addition, although multiple cases were designed, the explored parameter space remains limited and does not cover all possible cable loads, layouts, and material/aging conditions. Future work will expand the experimental matrix across diverse tunnel configurations and ventilation strategies, incorporate broader cable/material scenarios, and integrate enhanced diagnostics and validated models to improve generalizability and engineering applicability.

References

An, W. G., Ding, J., Zhang, Y., et al. 2024. Temperature distribution and extinction characteristics of cable fire in a narrow and long space under air pressure and sealing effects. *Safety and Environmental Engineering*.

Zhang, J. Q., Yan, X. D., Tan, T. T., et al. 2025. Influence of slope on fire spread characteristics in cable tunnels of pumped storage power stations. *Journal of Tsinghua University (Science and Technology)*.

Zhang, T. C., Wang, Z., Xu, F. X., et al. 2025. Study on fire spread behavior in cable trays of utility tunnels under different air pressures. *Journal of Safety Science and Technology*, 21(09): 13-20.

Zhao, Y. C., Zhu, G. Q., Gao, Y. J. 2018. Experimental study on smoke temperature distribution under different power conditions in utility tunnel. *Case Studies in Thermal Engineering*, 12: 69-76.

Liu, X. J., Xu, Z. D., Dai, J., et al. 2025. Study on the flame propagation and temperature distribution in utility tunnel: the spread effect of cable fire. *Applied Thermal Engineering*, 279(Part F): 128101.

An, W. G., Wang, X. S., Tang, Y. H., et al. 2021. Influence of cable inclination angle and longitudinal ventilation on temperature distribution during cable fire in utility tunnel. *Case Studies in Thermal Engineering*, 27: 101304.

Liang, K., Hao, X. F., An, W. G., et al. 2019. Study on cable fire spread and smoke temperature distribution in T-shaped utility tunnel. *Case Studies in Thermal Engineering*, 14: 100433.

Huang, X. J., Ding, H. L., Wang, M. 2024. Effects of space size and fire location on heat transfer in flame spread over electrical wire in a small tunnel. *Case Studies in Thermal Engineering*, 64: 105523.

Liu, M. Z., Chen, Y., Zhao, S. Z., et al. 2025. Experimental study on fire spread behavior of inclined dual cables in a narrow and long space. *Fire Science and Technology*, 44(06): 731-737.

Xu, D. S., Li, Y. F., Li, J. M., et al. 2025. Combustion characteristics and flame morphological evolution of double-layer cable fires in urban utility tunnels with various laying spacings. *Energy*, 315: 134324.

Xu, D. S., Li, Y. F., Li, J. X., et al. 2023. Evaluating the combustion and flame extension characteristics of cable fire in utility tunnels with spontaneous combustion scenarios: An experimental study. *Tunnelling and Underground*

Space Technology, 140: 105244.

An, W. G., Wang, T., Liang, K., et al. 2020. Effects of interlayer distance and cable spacing on flame characteristics and fire hazard of multilayer cables in utility tunnel. *Case Studies in Thermal Engineering*, 22: 100784.

Wang, J., Song, X. Y., Gao, D. M., et al. 2025. Ageing effect on the combustion characteristics of tunnel electric cables with various spacing distances. *Case Studies in Thermal Engineering*, 74: 106982.

Bai, Z. P. 2024. Burning characteristics of power cables with cone calorimeter. *Heliyon*, 10(3): e25103.

Zheng, X. Z., Cai, G. B., Guo, J., et al. 2023. Combustion characteristics and thermal decomposition mechanism of the flame-retardant cable in urban utility tunnel. *Case Studies in Thermal Engineering*, 44: 102887.

An, W. G., Tang, Y. H., Liang, K., et al. 2020. Study on temperature distribution and CO diffusion induced by cable fire in L-shaped utility tunnel. *Sustainable Cities and Society*, 62: 102407.

Wang, C. Z., Guo, D. P., Xu, B. Z., et al. 2025. Experimental study and numerical simulation of fire spread in urban cable tunnels. *Journal of Tsinghua University (Science and Technology)*, 65(03): 532-546.

Xu, D. S., Li, Y. F., Yang, Q. 2024. Research progress on cable fires in the electrical cabin of utility tunnels. *Fire Science and Technology*, 43(09): 1213-1217+1246.

Wang, T., An, W. G. 2023. Experimental study on flame spread and extinction over horizontal power cables under longitudinal ventilation in a utility tunnel. *Thermal Science and Engineering Progress*, 39: 101752.

Wang, T., Ding, J., Zhang, T. C., et al. 2024. Modelling of heat release rate of horizontal cable trays fire in long-narrow confined spaces. *Tunnelling and Underground Space Technology*, 150: 105831.

Liu Chang received his Ph.D. from Northeastern University and completed postdoctoral research at Tsinghua University. He currently serves as a Senior Engineer at the State Grid Electric Power Engineering Research Institute, specializing in safety science. His research has been recognized with the First Prize in the Science and Technology Progress Award from both the China Association of Work Safety and the China Occupational Safety and Health Association.